PHYSICAL REVIEW B **82**, 155309 (2010)

Anomalous transport in an *n*-type topological insulator ultrathin Bi_2Se_3 film

Toru Hirahara,[1,*] Yusuke Sakamoto,[1] Yasuo Takeichi,[2] Hidetoshi Miyazaki,[3] Shin-ichi Kimura,[3] Iwao Matsuda,[2] Akito Kakizaki,[2] and Shuji Hasegawa[1]

[1]*Department of Physics, University of Tokyo, 7-3-1 Hongo, Bunkyo-ku, Tokyo 113-0033, Japan*

[2]*Synchrotron Radiation Laboratory, ISSP, University of Tokyo, Kashiwa 277-8581, Japan*

[3]*UVSOR Facility, Institute for Molecular Science, Okazaki 444-8585, Japan*

(Received 20 July 2010; revised manuscript received 6 September 2010; published 5 October 2010)

We have performed *in situ* spin- and angle-resolved photoemission and *ex situ* magnetotransport measurements on ultrathin topological insulator Bi_2Se_3 films. The surface states deviate from a simple isotropic Dirac fermion due to hexagonal warping effects and their spin helical nature has been verified. In addition, the bulk states also cross the Fermi level, showing that the films are actually *n* doped. However, the temperature dependence of the film resistivity was insulating and saturated below 35 K. Furthermore, the magnetoresistivity changed drastically as the sample was cooled down and showed an anomaly near zero field below 20 K. The possible origin of this peculiar behavior and the nature of the carriers involved are discussed in comparison with the results for nonmetallic bulk samples.

DOI: 10.1103/PhysRevB.82.155309 PACS number(s): 75.70.Tj, 73.20.−r, 73.61.Ng

I. INTRODUCTION

Topological insulators have attracted much attention from a wide variety of researchers in condensed-matter physics. Along with the quantum spin Hall state in two dimensions, they are mathematically characterized by the so-called Z_2 topological number.[1] While the bulk is insulating, there is a metallic edge or surface state which is topologically protected and hence robust against weak perturbation or disorder, and many exotic quantum phenomena are expected to occur associated with their topologically nontrivial nature.[2,3] Angle-resolved photoemission spectroscopy (ARPES) measurements have directly shown the presence of such surface states and their spin helical nature have been resolved for materials such as $Bi_{1-x}Sb_x$, Bi_2Se_3, and Bi_2Te_3.[4–7]

In principle, when the sample is cooled down to low temperatures, the insulating bulk carriers will freeze out and only the metallic surface states should contribute to the physical properties. But it has been known that some unwanted doping occurs, and in reality it is difficult to make the bulk "insulating." ARPES studies have shown that naturally grown stoichiometric samples are actually *n*-type due to inevitable defects or substitutions.[4,7] Many attempts have been made to perform an opposite doping with intentional substitution which have partly been successful.[8] Alternatively, the same surface states were fabricated on an ultrathin film which highly enhanced the surface/volume ratio.[9]

However, there is still no clear-cut conclusion whether the surface-state conductivity is actually dominating the transport phenomena despite quite a large number of studies. Many Shubnikov-de Haas oscillation measurements have shown the presence of a bulk Fermi surface even for very high-purity insulating samples.[10–15] This is partly due to the different environment in which ARPES and transport measurements are performed. In ARPES, the experiments are all performed in ultrahigh-vacuum conditions where the crystals are cleaved *in situ* prior to the measurement. In contrast, transport measurements are basically performed *ex situ* in air. Whether the same surface states are present in both environment is an open question; some reports have been made on the oxidation process of these materials.[16] Therefore, ideally transport measurements should also be done *in situ* if we really want to know the surface-state conductivity. Previously we have fabricated ultrathin $Bi_{1-x}Sb_x$ alloy films and performed *in situ* transport measurements by changing the thickness which showed clear crossover from a film-dominant to a surface-state-dominant conductivity as the film thickness was reduced.[9] The next step is an *in situ* conductivity measurement at low temperature and under magnetic field to clarify the Fermi surface of the carriers and compare with that obtained by ARPES. Such system is now under construction.

In the present work, we have fabricated ultrathin Bi_2Se_3 films *in situ* (80 Å thick) and measured its electronic structure with ARPES as well as spin-resolved ARPES (SARPES). Then the sample was taken out to air and *ex situ* magnetotransport measurements were performed. Under the assumption that the bulk (film) states do not change drastically even though it is not clear how the surface states will be changed by exposition to air, we should be able to obtain some information concerning the bulk properties. From ARPES, we found the same surface states as the bulk single crystals exist on the films. The surface Fermi surface was hexagonal due to the hexagonal warping effect although believed to be circular. The spin structure was directly mapped with SARPES, showing the expected helical structure. The bulk (film) state bands also crossed the Fermi level, indicating that the films are *n* doped. However, despite the fact that both the bulk and surface states are metallic, the temperature dependence of the film conductivity showed an insulating behavior and saturated below 35 K. From the estimated mobility this could not be ascribed to the poor film quality. Furthermore, the magnetoresistivity was also peculiar, showing a large cusp near zero field below 20 K. The origin of these anomalous behavior and carrier properties are discussed by comparing with transport studies of bulk crystals. Our results strongly point to the importance to perform *in situ* magnetotransport measurements.

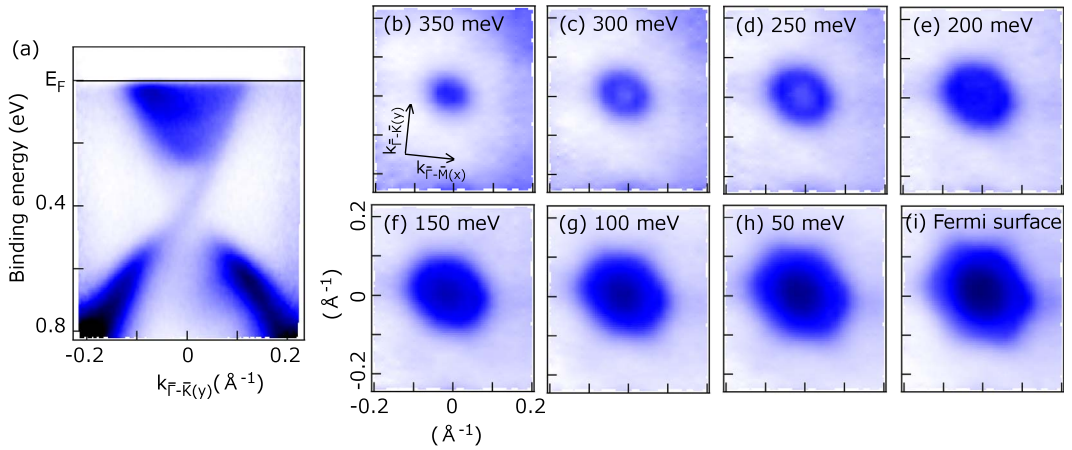

FIG. 1. (Color online) (a) *E-k* band dispersion image of an 8 QL ultarthin Bi_2Se_3 film along the $\bar{\Gamma}$-$\bar{K}$ direction near the $\bar{\Gamma}$ point. [(b)–(i)] Constant energy contour mapping of an 8 QL ultarthin Bi_2Se_3 film for respective energies.

II. EXPERIMENTAL

The ultrathin Bi_2Se_3 films were fabricated *in situ* in a method similar to the report of Ref. 17. First, a clean Si(111)-7×7 surface was prepared on an *n*-type substrate (P-doped, 1–10 Ω cm at room temperature) by a cycle of resistive heat treatments. The Si(111)$\beta\sqrt{3}\times\sqrt{3}$-Bi surface was formed by 1 ML (7.83×10^{14} cm^{-2}) of Bi deposition on the 7×7 surface at 620 K monitored by reflection high-energy electron diffraction (RHEED). Then Bi was deposited on the $\beta\sqrt{3}\times\sqrt{3}$-Bi structure at ~400 K under a Se-rich condition. Such a procedure is reported to result in a smooth epitaxial film formation with the stoichiometric ratio of Bi:Se=2:3.[17] It is also known that the minimum film thickness that can be achieved in this method is one quintuple layer (1 QL=10 Å), and the films grow QL-by-QL. We have carefully checked the film thickness by monitoring the spot intensity oscillation of the RHEED pattern.[18]

The ARPES experiments were performed at BL-5U of UVSOR using an electron analyzer of MBS-Toyama A-1. The energy and the angular resolutions were 20 meV and 0.2°, respectively. The photon energies used were $h\nu$=20–24 eV and the measurements were done at 10 K. The spin-resolved ARPES measurements were performed at BL-19A of KEK-PF with a SPECS Phoibos-150 equipped with a homemade high-yield spin polarimeter using spin-dependent very-low-energy electron diffraction.[19] A He lamp (He Iα $h\nu$=21.2 eV) was used as the excitation source and the SARPES spectra were recorded at 150 K with the energy and angle resolutions of 30 meV and 0.7°, respectively. The effective Sherman function in this experiment was 0.3 as calibrated by the spin-polarized secondary electrons from a standard Ni sample.

After the SARPES measurement, the sample was exposed to air and transferred for *ex situ* transport studies. Then probes were attached to the films and magnetotransport measurements were performed in the temperature range of 5–250 K and under magnetic field as high as 9 T in the Physical Properties Measurement System (PPMS) system (Quantum Design) at the Cryogenic Research Center, University of Tokyo.

III. RESULTS AND DISCUSSION

A. Electronic properties: Hexagonal warping effect and helical spin structure

First we describe the electronic property of the 8-QL-thick ultrathin Bi_2Se_3 film. Figure 1(a) shows the band dispersion image near the Fermi level in vicinity of the $\bar{\Gamma}$ point along the $\bar{\Gamma}$-$\bar{K}$ direction (*y* direction). The strong intensity features just below the Fermi level E_F and those below 0.5 eV correspond to the bulk states. The broad features of this bulk conduction band are quite similar to those found in the bulk crystal case.[4] On the other hand, the states with linear dispersion around E_B=0.4 eV at $\bar{\Gamma}$ correspond to the surface states with Dirac-type linear dispersion. The positive wave-number side of the bands seems to have a higher photoemission intensity than the negative side, which is presumably due to the circularly polarized photons used in the measurements. By changing the photon helicity, the intensity distribution reversed.

It can be seen that both the surface state and the bulk states are metallic with the Dirac point about 0.4 eV below E_F. This clearly shows that the ultrathin Bi_2Se_3 films are electron doped although ideally only the surface states should be metallic, which has been attributed to inevitable Se site defects inside the crystal.[4,8] In Bi_2Se_3, Bi has +3 valency and donates three electrons per atom while Se has −2 valency and accepts two electrons per atom. Therefore when there are less Se than Bi, it becomes an *n*-type semiconductor. Our results indicate that such unwanted bothersome doping is also present for the ultrathin films. From the obtained Fermi wave number of the bulk (film) states, the carrier density inside the film is roughly estimated as ~10^{-19} cm^{-3} assuming a spherical Fermi surface. The defect density of Se is estimated to be in the same order of magnitude.

Now let us look more closely into the surface-state properties. Figures 1(b)–1(i) show the results of the constant energy contour (CEC) mapping at (b) E_B=350 meV, (c) 300 meV, (d) 250 meV, (e) 200 meV, (f) 150 meV, (g) 100 meV, (h) 50 meV, and that at (i) the Fermi level, respectively. The features for (e)–(i) above 200 meV contain the

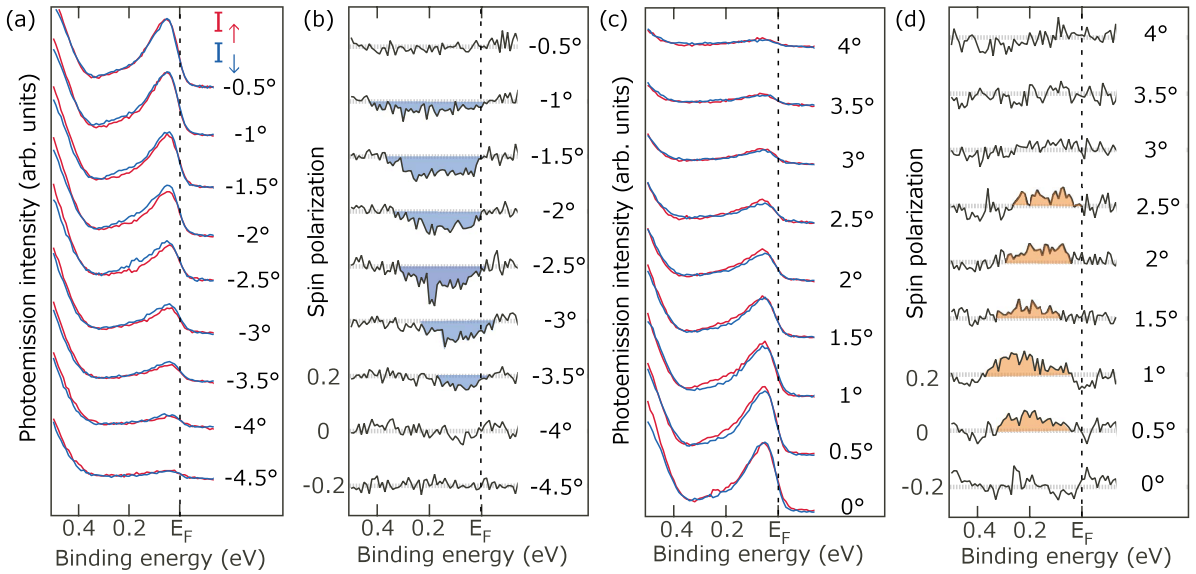

FIG. 2. (Color online) Spin-resolved ARPES spectra of an 8 QL ultrathin Bi_2Se_3 film along the $\bar{\Gamma}$-$\bar{M}$ direction [(a) and (c)] and the spin-polarization curves deduced from them [(b) and (d)]. The spin orientation is along the $\bar{\Gamma}$-$\bar{K}$ direction [y direction, red (light gray) for $+y$ and blue (dark gray) is for $-y$, respectively].

bulk states near $\bar{\Gamma}$ as has been discussed above. Whereas the CEC at higher binding energies in (b)–(d) are mostly circular and isotropic, those near E_F in (e)–(i) become distorted and are rather hexagonal. Although results of Fermi-surface mapping has been reported in previous reports of bulk single crystal Bi_2Se_3,[4] this hexagonal feature has never been clearly shown. In contrast such change in the shape of the CEC has been observed for Bi_2Te_3,[7] which has been explained as a hexagonal warping effect (HWE).[20] The Hamiltonian of the surface states can be expressed as

$$H(k) = E_0 + v(k_x\sigma_y - k_y\sigma_x) + \frac{\lambda}{2}(k_+^3 + k_-^3)\sigma_z, \qquad (1)$$

where the first two terms describe the usual linear dispersion (v is the velocity) and the last term describing the cubic spin-orbit coupling is responsible for the HWE. σ_i is the so-called pseudospin which is proportional to the real spin s_i and λ is the parameter governing the strength of the HWE. It is written in Ref. 20 that when $E > 0.69v/\sqrt{\lambda/v}$, the edge of the hexagon curves inward so that the CEC becomes more snowflakelike. Since the CEC shown in Figs. 1(b)–1(i) do not show such feature, we assume that the Fermi surface of Fig. 1(i) corresponds to $E = 0.69v/\sqrt{\lambda/v}$. From comparison of Fig. 1(i) to Fig. 2(a) of Ref. 20, we obtain $\lambda = 95$ eV Å^3 using $v = 4.6 \times 10^5$ m/s.[18] Then the Dirac point is obtained as $0.69 \times v/\sqrt{\lambda/v} = 0.37$ eV, which is in good agreement with the band dispersion shown in Fig. 1(a) (0.40 eV). The value of λ for Bi_2Te_3 was 250 eV Å^3, much larger than the present case. While a clear-cut explanation of this large difference cannot be given, it may be due to the fact that bulk electronic structure is more anisotropic for Bi_2Te_3 compared to Bi_2Se_3. More work is needed to obtain a generic understanding.

An important aspect of the topological surface states is that they have a helical spin structure, i.e., the spin orientation is locked to the wave number due to the Rashba effect.[5] This has directly been proven for Bi_2Te_3 for one momentum dispersion curve[5] but a comprehensive measurement is lacking. Therefore, we have carried out SARPES measurements on the same 8-QL-thick ultrathin Bi_2Se_3 film formed *in situ* in another photoemission system. Figures 2(a) and 2(c) show the SARPES spectra ($I_\uparrow$,$I_\downarrow$) near the $\bar{\Gamma}$ point along the $\bar{\Gamma}$-$\bar{M}$ direction (x direction) for (a) negative and (c) positive emission angles, respectively, and Figs. 2(b) and 2(d) show the corresponding spin-polarization curves $P = \frac{I_\uparrow - I_\downarrow}{I_\uparrow + I_\downarrow}$. The spin orientation is in the $+y$ [red (light gray)] ($-y$ [blue (dark gray)]) direction. As we have seen in Fig. 1(a), the photoemission intensity for the bulk states are much stronger than that of the surface states and it is really difficult to resolve the two in the energy distribution curves of Figs. 2(a) and 2(c). However, if we look carefully at $I_\uparrow$ and $I_\downarrow$, we notice that $I_\uparrow < I_\downarrow$ for negative angles, $I_\uparrow = I_\downarrow$ just near normal emission, and $I_\uparrow > I_\downarrow$ for positive angles near the Fermi level. This can also be noticed by the hatched areas in the spin-polarization curves of Figs. 2(b) and 2(d). The spin-polarized states seem to disperse toward E_F as they pull off from normal emission, which is similar to the surface-state band dispersion in Fig. 1(a). We believe that this is representing the helical nature of the spin-split surface states. The obtained spin-polarization values are ~10% at maximum, which is very small probably due to the strong intensity of the non-polarized bulk state close by. It may also be due to the fact that there is mixing between the surface and bulk states. Another effect may come from a technical problem concerning the He Iβ and/or He II radiation enhancing the background of the spectra.

We would also like to comment on the influence of HWE on the spin orientation. As can be seen from Eq. (1), the

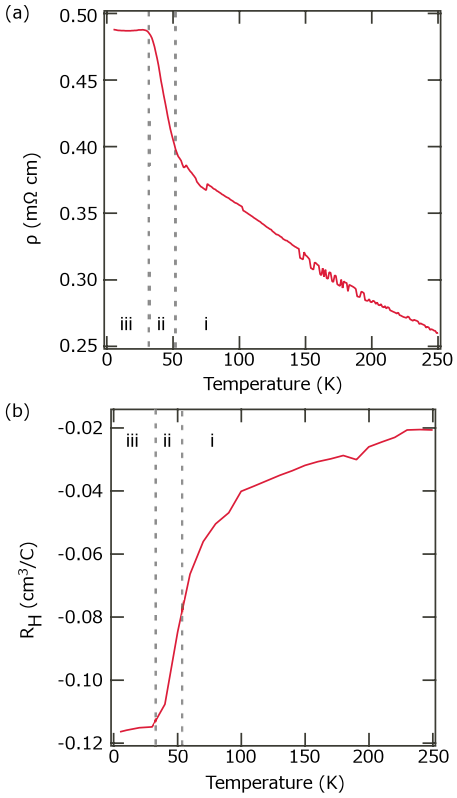

FIG. 3. (Color online) The temperature dependence of the (a) film resistivity ρ and (b) the Hall coefficient R_H for the 8 QL ultrathin Bi_2Se_3 film.

cubic terms couples to the z (out-of-plane) component of the spin, meaning that there should be out-of-plane spin polarization observed in addition to the in-plane components for some directions in the surface Brillouin zone. Unfortunately in our SARPES experimental setup it is impossible to measure the z component near normal emission and no investigation can be made. In Ref. 5, the authors have shown that there is presumably a weak spin polarization observed for the z components in Bi_2Te_3. Further high-resolution, high-efficiency SARPES measurements will unravel the precise spin vectors of the surface states.

B. Magnetotransport properties: Anomalous temperature and magnetic field dependence

In the previous section, we have found that the ultrathin Bi_2Se_3 films fabricated *in situ* are *n* doped with both the bulk and surface states crossing the Fermi level. When we expose them to air for transport measurements the surface states should be affected somehow. However, it is likely that the bulk carriers will maintain their metallicity because it cannot be anticipated that the whole film will be destroyed considering that the film thickness is ~80 Å. It has been reported for Bi_2Te_3, that only one or two QL will be oxidized.[16]

Figure 3(a) shows the temperature dependence of the film resistivity $\rho(\rho_{xx})$. In contrast to the metallic conduction expected from the electronic structure, ρ increases as the temperature is lowered which is a semiconducting or an insulating behavior. In fact by carefully inspecting Fig. 3(a), it seems that the there are three different regions: (i) 50–250 K where the resistivity rises gradually, (ii) 35–50 K where the resistivity rises steeply, and (iii) below 35 K where the resistivity is nearly constant. For every region, ρ is in the order of 10^{-1} mΩ cm. This change can basically be correlated with the change in the carrier density, which can be recognized from the temperature dependence of the Hall coefficient R_H, as shown in Fig. 3(b). R_H was determined from the slope of the ρ_{xy}-B curves. The carrier density (assuming a one-band model) is 3.1×10^{20} cm^{-3}, 8.7×10^{19} cm^{-3}, and 5.5×10^{19} cm^{-3} at 250 K, 50 K, and 5 K, respectively. The carrier density at 5 K is roughly similar to the value estimated from the area of the Fermi surface. The values of ρ and R_H are in good accordance with those of bulk Bi_2Se_3 crystals showing metallic conduction.[5,11] Furthermore, the Hall mobility $\mu_H=R_H\cdot\sigma(\sigma=\sigma_{xx}=\frac{\rho_{xx}}{\rho_{xx}^2+\rho_{xy}^2})$ is 250 cm^2/V s at 5 K, which is only slightly smaller than the values shown in Ref. 11 for the metallic bulk crystals with similar carrier density.[21] However, we emphasize that the temperature dependence of Fig. 3(a) is *nonmetallic* which is inconsistent with the metallic band structure measured *in situ*. It is unlikely that this insulating conduction is due to some localization effect of the poor film quality since the mobility is in the same order of magnitude as bulk materials with similar carrier density. Although we cannot make a definite conclusion, this may be due to the change in the band dispersion by exposing the film to air; the bulk bands themselves may have become insulating or some unknown additional carriers that play a key role in the transport can be present. Actually this temperature dependence of ρ is qualitatively rather similar to that of the nonmetallic $Ca_xBi_{2-x}Se_3$ reported in Ref. 14, showing saturation at low temperatures instead of a divergence expected for an usual insulator. We have tried to fit the curve of Fig. 3(a) to an activation type function $\rho=\rho_0\exp(\frac{E_g}{2k_BT})$. Only region (ii) could be well fitted, giving $E_g=5$ meV. Although the meaning of this activation energy is unclear, it can be concluded that region (i) is not an usual carrier activation process and the origin of the carrier density decrease in Fig. 3(b) is not straightforward.

In order to gain further insight into the above anomalous behavior, we have performed magnetotransport measurements. Figures 4(a) and 4(b) show the magnetic field dependence of ρ when the field is applied (a) perpendicular or (b) parallel to the sample surface, respectively. It can be recognized that the magnetotransport behavior changes drastically among the different temperature regimes discussed above; in region (i) (above 50 K), there is a negative magnetotransport behavior first at low fields which turns back to a positive one at high fields in the out-of-plane direction while it is positive for both low and high fields in the in-plane direction. For the data at 50 K [region (ii)], there seems to be no anisotropy in the applied field direction and the magnetotransport reaches as high as 120% at ±9 T. The most remarkable anomalous behavior is found in region (iii) (below 35 K) while $\rho(B)$ for the in-plane direction can be explained classically, a quadratic dependence at low fields and saturation at high fields [Fig. 4(b)], the curves for the 5, 10, and 20 K in Fig. 4(a) show a sharp cusp near zero field and the magnetoresistivity increases at high fields with no saturation. The cusp feature

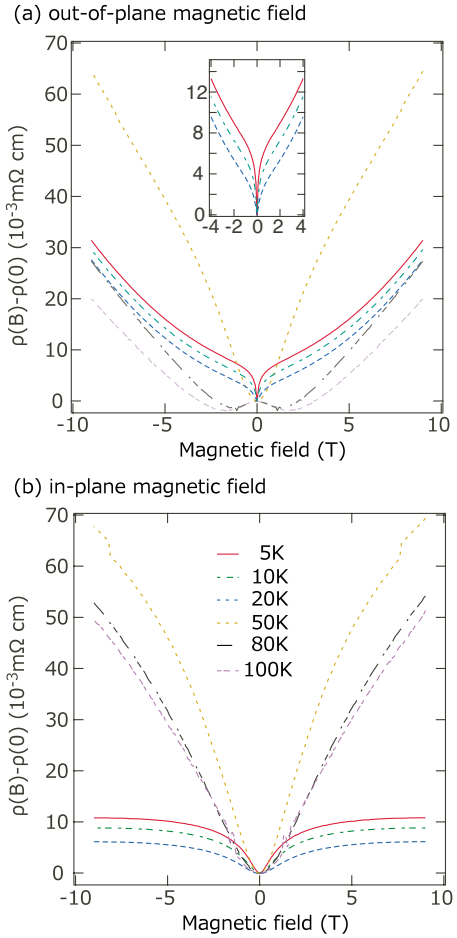

FIG. 4. (Color online) The magnetic field dependence of the resistivity ρ for the 8 QL ultrathin Bi_2Se_3 film with the magnetic field applied in the (a) out-of-plane direction and (b) in-plane direction at respective temperatures. The inset in (a) shows the enlarged curves at the measurement temperatures of 5, 10, and 20 K.

becomes prominent as the temperature is lowered which can be recognized from the inset in Fig. 4(a).

In fact, such sharp cusp features have been previously reported for the nonmetallic $Ca_xBi_{2-x}Se_3$ bulk crystal in Ref. 14. They have even found that by cooling the sample even further down to 0.3 K, a signature of unconventional quantum interference can be seen in a macroscopic sample from the oscillatory magnetic field dependence of ρ. Even though we do not see such oscillation due to the limitation of cooling, the observation of this singularity near zero field indicates that similar types of carriers are also involved in our ultrathin films. This is also evidenced by two other facts: (1) near the cusp ρ vs B follows a logarithmic behavior [Fig. 5(a)], and (2) the conductivity σ vs B also follows a logarithmic behavior [Fig. 5(b)], both of which have been reported in Ref. 14. The latter is suggestive of an antilocalization in a two-dimensional system. By fitting σ at 5 K to

$$\sigma(B) - \sigma(0) = -\frac{e^2}{h} A \log B, \tag{2}$$

where A is the coefficient in the order of $1/2\pi$ related to the spin and orbital contributions to the weak localization,[22] we

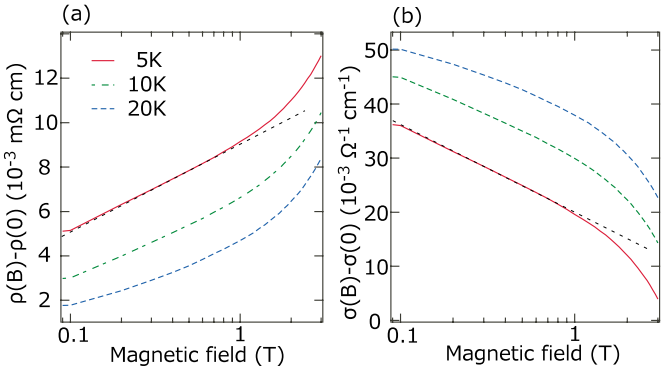

FIG. 5. (Color online) (a) The magnetic field dependence of the resistivity ρ for the 8 QL ultrathin Bi_2Se_3 film plotted as a function of log B for the 5, 10, and 20 K curves of Fig. 4(a). (b) The magnetic field dependence of the conductivity σ as a function of log B for the 5, 10, and 20 K curves of Fig. 4(a). The dashed lines near the curve of 5 K show a fitting to a linear function.

obtain $A=440$. This large discrepancy from theory indicates that this phenomenon cannot be considered as weak antilocalization in a two-dimensional system and the origin of this anomaly is unclear.

As discussed above, the similarity concerning the temperature and magnetic field dependence of the resistivity between the samples studied in nonmetallic bulk samples in Ref. 14 and our ultrathin films suggests that the same carriers are involved in the transport phenomena at low temperatures. One possibility may be the surface states: since the areal carrier density for the bulk (film) and surface are comparable ($\sim 10^{13}$ cm^{-2}), surface-state conductivity may be possible depending on mobility. Some reports have been made on enhanced (Ref. 11) or reduced (Ref. 23) scattering for the topological surface states compared to the bulk states. But as we have emphasized before, there is no guarantee that the surface states can survive in ambient condition. It has also been reported that some kind of a space-charge layer may be present due to band-bending effect which can be responsible for these anomaly.[14,15] Such carriers may also be the origin of the time-dependent doping phenomenon found in ARPES studies.[5] Furthermore in a recent photoemission study of Bi_2Se_3 films formed on graphene/SiC, the authors have shown that band bending can also be derived from the substrate and even influence the surface-state dispersion.[24] They have even found temperature dependence in the band bending (due to surface photovoltage effects) although the dispersions themselves (whether the bands are metallic or semiconducting, gap size, etc.) seem to be independent of temperature. Since the thickness of our sample is ~80 Å, carriers at such space-charge layer can dominate the film conductivity. Similarly since the bulk carrier density is very small in Ref. 14, the space-charge region will extend inside the crystal and may dominate the transport phenomenon even for the bulk crystal. But we should also be aware that the actual values of ρ and carrier density are one to two orders of magnitude larger and the mobility is one to two orders smaller in our case compared to the bulk nonmetallic samples, and whether this anomalous transport behavior can really be regarded the same remains uncertain. However, we

still think this anomalous behavior is most likely a bulk property. To precisely determine the intriguing properties that each carriers possess (surface states and bulk or film states), it is really important to perform transport measurements in ultrahigh-vacuum conditions where the surface states are known to be present for sure.

IV. CONCLUSION

In conclusion, we have performed *in situ* spin- and angle-resolved photoemission measurements and *ex situ* magnetotransport measurements on ultrathin Bi_2Se_3 films. We clearly observed the spin helical nature of the metallic surface states as well as the deviation from a circular Fermi surface due to the hexagonal warping effect. The bulk bands also crossed the Fermi level, showing that they are actually *n* doped. In contrast to the metallic electronic structure, the temperature dependence of the film resistivity was insulating and saturated below 35 K. Furthermore, the magnetoresistivity showed an anomalous behavior below 20 K having a cusp near zero field. The results have been compared with the bulk case and its possible origin has been discussed. Our results suggest that even when the transport properties are insulating, the possibility of a metallic bulk band structure should be considered. *In situ* magnetotransport measurements will provide further interesting properties and unravel the topologically protected nature of the surface states.

Note added. During the course of our submission, we became aware of a similar work reporting the hexagonal warping effects in bulk Bi_2Se_3 crystals.[25]

ACKNOWLEDGMENTS

We acknowledge Takenori Fujii at the Cryogenic Research Center, University of Tokyo for performing the transport measurements, assistance from Akinori Nishide in the SARPES measurement, and Taichi Okuda for his valuable comments concerning the data interpretation. This work has been supported by Grants-In-Aid from Japanese Society for the Promotion of Science. The ARPES experiments were performed under the proposal numbers of UVSOR 21-524, 22-521, and PF 2009G006.

*hirahara@surface.phys.s.u-tokyo.ac.jp

[1] C. L. Kane and E. J. Mele, Phys. Rev. Lett. **95**, 146802 (2005).
[2] X.-L. Qi, R. Li, J. Zang, and S.-C. Zhang, Science **323**, 1184 (2009).
[3] L. Fu and C. L. Kane, Phys. Rev. Lett. **100**, 096407 (2008).
[4] Y. Xia, D. Qian, D. Hsieh, L. Wray, A. Pal, H. Lin, A. Bansil, D. Grauer, Y. S. Hor, R. J. Cava, and M. Z. Hasan, Nat. Phys. **5**, 398 (2009).
[5] D. Hsieh, Y. Xia, D. Qian, L. Wray, J. H. Dil, F. Meier, J. Osterwalder, L. Patthey, J. G. Checkelsky, N. P. Ong, A. V. Fedrov, H. Lin, A. Bansil, D. Grauer, Y. S. Hor, R. J. Cava, and M. Z. Hasan, Nature (London) **460**, 1101 (2009).
[6] A. Nishide, A. A. Taskin, Y. Takeichi, T. Okuda, A. Kakizaki, T. Hirahara, K. Nakatsuji, F. Komori, Y. Ando, and I. Matsuda, Phys. Rev. B **81**, 041309(R) (2010).
[7] Y. L. Chen, J. G. Analytis, J.-H. Chu, Z. K. Liu, S.-K. Mo, X. L. Qi, H. J. Zhang, D. H. Lu, X. Dai, Z. Fang, S. C. Zhang, I. R. Fisher, Z. Hussain, and Z.-X. Shen, Science **325**, 178 (2009).
[8] Y. S. Hor, J. G. Checkelsky, D. Qu, N. P. Ong, and R. J. Cava, arXiv:1006.0317 (unpublished).
[9] T. Hirahara, Y. Sakamoto, Y. Saisyu, H. Miyazaki, S. Kimura, T. Okuda, I. Matsuda, S. Murakami, and S. Hasegawa, Phys. Rev. B **81**, 165422 (2010).
[10] A. A. Taskin and Y. Ando, Phys. Rev. B **80**, 085303 (2009).
[11] N. P. Butch, K. Kirshenbaum, P. Syers, A. B. Sushkov, G. S. Jenkins, H. D. Drew, and J. Paglione, Phys. Rev. B **81**, 241301(R) (2010).
[12] K. Eto, Z. Ren, A. A. Taskin, K. Segawa, and Y. Ando, Phys. Rev. B **81**, 195309 (2010).
[13] A. Taskin, K. Segawa, and Y. Ando, arXiv:1001.1607 (unpublished).
[14] J. G. Checkelsky, Y. S. Hor, M.-H. Liu, D.-X. Qu, R. J. Cava, and N. P. Ong, Phys. Rev. Lett. **103**, 246601 (2009).
[15] J. G. Analytis, J.-H. Chu, Y. Chen, F. Corredor, R. D. McDonald, Z. X. Shen, and I. R. Fisher, Phys. Rev. B **81**, 205407 (2010).
[16] H. Bando, K. Koizumi, Y. Oikawa, K. Daikohara, V. A. Kulbachinskii, and H. Ozaki, J. Phys.: Condens. Matter **12**, 5607 (2000).
[17] G. Zhang, H. Qin, J. Teng, J. Guo, X. Dai, Z. Fang, and K. Wu, Appl. Phys. Lett. **95**, 053114 (2009).
[18] Y. Sakamoto, T. Hirahara, H. Miyazaki, S. I. Kimura, and S. Hasegawa, Phys. Rev. B **81**, 165432 (2010).
[19] T. Okuda, Y. Takeichi, Y. Maeda, A. Harasawa, I. Matsuda, T. Kinoshita, and A. Kakizaki, Rev. Sci. Instrum. **79**, 123117 (2008).
[20] L. Fu, Phys. Rev. Lett. **103**, 266801 (2009).
[21] At low temperature, the carrier mean-free path may be determined by the film thickness, which may have influence on the measured mobility. However, such surface/interface scattering as well as impurity/defect scattering should not show significant temperature dependence and cannot be the sole reason for the nonmetallic temperature dependence.
[22] S. Hikami, A. I. Larkin, and Y. Nagaoka, Prog. Theor. Phys. **63**, 707 (1980).
[23] D.-X. Qu, Y. S. Hor, J. Xiong, R. J. Cava, and N. P. Ong, Science **329**, 821 (2010).
[24] Y. Zhang, K. He, C.-Z. Chang, C.-L. Song, L.-L. Wang, X. Chen, J.-F. Jia, Z. Fang, X. Dai, W.-Y. Shan, S.-Q. Shen, Q. Niu, X.-L. Qi, S.-C. Zhang, X.-C. Ma, and Q.-K. Xue, Nat. Phys. **6**, 584 (2010).
[25] K. Kuroda, M. Arita, K. Miyamoto, M. Ye, J. Jiang, A. Kimura, E. E. Krasovskii, E. V. Chulkov, H. Iwasawa, T. Okuda, K. Shimada, Y. Ueda, H. Namatame, and M. Taniguchi, Phys. Rev. Lett. **105**, 076802 (2010).